

Chapter 4

Linkage of sediment indigenous properties with microbial parameters in two laterally deposited Late Quaternary sediment cores of the Mahi River basin: A case study from Rayka and Rampura

“All the power is within you, you can do anything and everything. Believe in that; don’t believe that you are weak, stand up and express the divinity within you.”

- Swami Vivekananda

4.1 Introduction

River ecosystems and their floodplains have great economic importance and can be viewed as open ecosystems as they integrate with horizontal, vertical, and lateral hierarchical arrangements via hydrologic and geomorphic processes occurring within a temporal hierarchy (Ward 1989). River terraces (representing the former level of the floodplains) have been recognized as sinks and sources of older sediments that mobilized from upstream catchments and deposited as stratigraphic sequences (lithofacies) over the course of geologic time. On the broader range, vertical stratigraphic sequences observed at river terraces possess complex geological features involving distinctive lithological, geochemical and textural characteristics depending on their depositional sources and parent materials. However, at a smaller scale, each stratum and each location comprise relatively constant physical and chemical properties (Ghiorse and Wilson 1988). Furthermore, natural floodplain sediment deposits also serve as a reservoir of river borne nutrients (i.e. particulate organic matters and inorganic nutrients) depending on their geochemical and textural characteristics which in turn affects nutrient dynamics and the nature and activities of indigenous microbial assemblages (Besemer et al. 2005; Lowell et al. 2009; Bouwman et al. 2013). A determination of abiotic factors responsible for shaping microbial characteristics is a fundamental aspect for understanding ecosystem functioning and managing soil/sediment health (Doran and Zeiss 2000; Baritz et al. 2018; Shang et al. 2021). However, this knowledge is poorly understood for semiarid Late Pleistocene river terrace sedimentary ecosystems.

A previous study on the microbiological characteristics in association with physicochemical properties of soils/sediments of the Mahi River basin was restricted to upper surface layers and exposed cliff alluvial deposits (Subrahmanyam et al., 2011a; 2011b; 2021). Surface and exposed sediments possess distinct physicochemical characteristics than buried subsurface soils and sediments as they are continually undergo erosion and directly connected with the atmospheric condition. Further, earlier chapter of this study explained correlation between microbial and sediment physicochemical parameters in the estuarine core sediment deposits of Late Pleistocene to Middle Holocene age lie at younger terrace surface of the Mahi River basin (refer section 1.7). Estuarine sediment deposits have transitional characteristics between fluvial and marine sediments and therefore comprise distinguish sediment

physicochemical characteristics than fluvial sediment deposits. In this chapter, an attempt was made to understand the correlation of physicochemical attributes with microbial parameters in two laterally deposited sediment core profiles that lie upstream region of the river and represent an older terrace surface of the Mahi River basin (refer section 1.7). These two core profiles largely comprised Late Pleistocene fluvial sediment deposits. The linkage between sediment physicochemical and microbial properties (includes enzyme activities involved in C, N, P, and S cycling, gene abundance and culturable counts) was determined within these two core profiles to identified key environmental parameters that correlate with microbial parameters. Analysis of two laterally deposited fluvial sediment core profiles provides insight into discrepancy of geological and microbial characteristics in both horizontal and vertical directions together with the linkage between microbial and geological parameters should help future investigations for microbial mediated improvement in sediment quality or health of the region via modifying identified environmental parameters that correlated with microbial parameters.

4.2 Results

4.2.1 Description of Rayka (RYD) and Rampura (RMD) core location and stratigraphic sequences observed within RYD and RMD cores

The Rayka core location (RYD) is ~0.2 km away from the Mahi River whereas the Rampura core location (RMD) is ~1.8 km away from the Mahi River and the latter is located near the Mini River (Fig. 4.1; also refer section 2.1). Mini River is a tributary of the Mahi River which is subjected to disposal of treated industrial effluents of the Nandesari industrial estate (Subrahmanyam et al. 2016). Further, RYD and RMD core locations lie on the older terrace of the Mahi River basin which is located 38 m above sea level (masl) and 27 masl respectively (Fig. 4.1). Both cores were provided laterally extended (~7.2 km apart from each other; refer section 2.1) Late Quaternary sediment sequences deposited during Late Pleistocene period (Juyal et al. 2000; Maurya et al. 2000). Representative photographs of split core liner showing the lithology of sediments present within RYD and RMD cores are depicted in Fig. A-IV (Appendix). The lithofacies observed in the RYD and RMD cores based on grain size distribution analysis and physical examination are shown in Fig. 4.2. Lithofacies identified in RYD and RMD cores are found to be composed mainly of fluvial and aeolian sediment

deposits. These sequences show silt clay horizons, aeolian sandy horizons, distinct gravelly horizons, and four intercalated distinct palaeosols (Fig. 4.2). Among the four palaeosols, three are brown color palaeosols present in the middle or lower part of the core profiles while one is red color palaeosol present in the uppermost part of both vertical cores (Fig. 4.2). The red palaeosol [dated 40 ± 10 ka; Juyal et al. (2000)] serves as a marker horizon for correlating stratigraphic sequences observed at laterally deposited sediments of the Mahi river Basin (Maurya et al. 2000). Hence, stratigraphic sequences observed within RYD and RMD cores were correlated with respect to red palaeosol as shown in Fig. 4.2. The uppermost part of both vertical cores is composed of aeolian deposits of Holocene age and is followed by fluvial deposition of Pleistocene age [as per Juyal et al. (2000)]. In the RYD core profile, the aeolian horizon presents up to 4.8 m thickness while in the RMD core profile, the aeolian deposit was only 1 m thick. Fluvial sediment sequences observed above red palaeosol in the RMD core are distinctive to the RMD core and not observed within the RYD core. The thickness of the red palaeosol also differed in the two core profiles (Fig. 4.2).

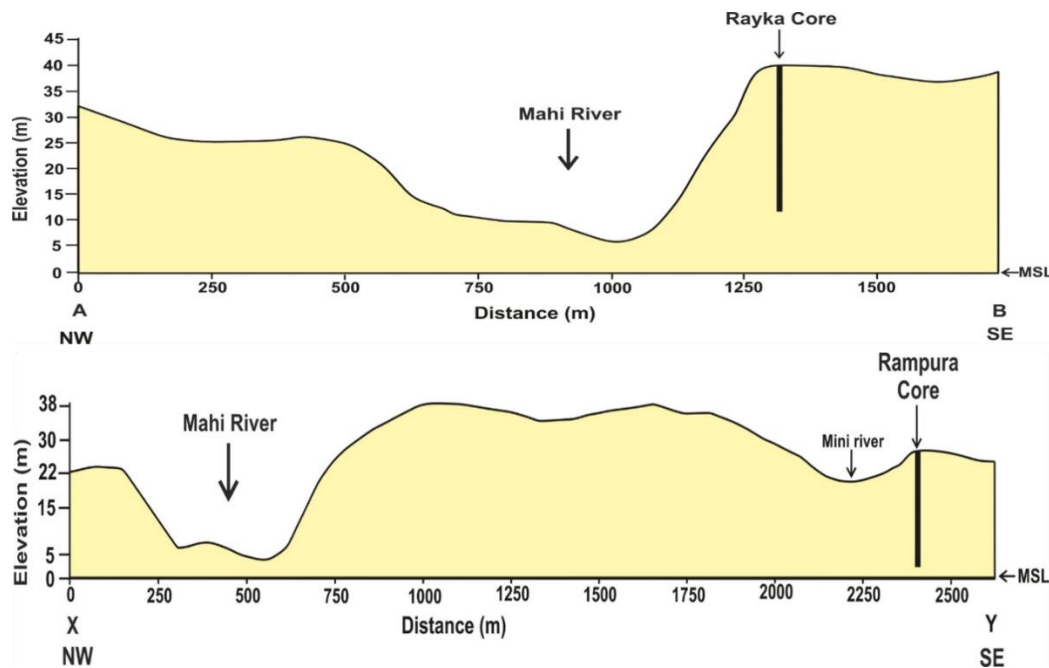


Figure 4.1: Cross-section of RYD and RMD core drilling sites. The distance of the core drilling site from the river channel, core depth from the ground surface with respect to mean sea level (MSL) are indicated.

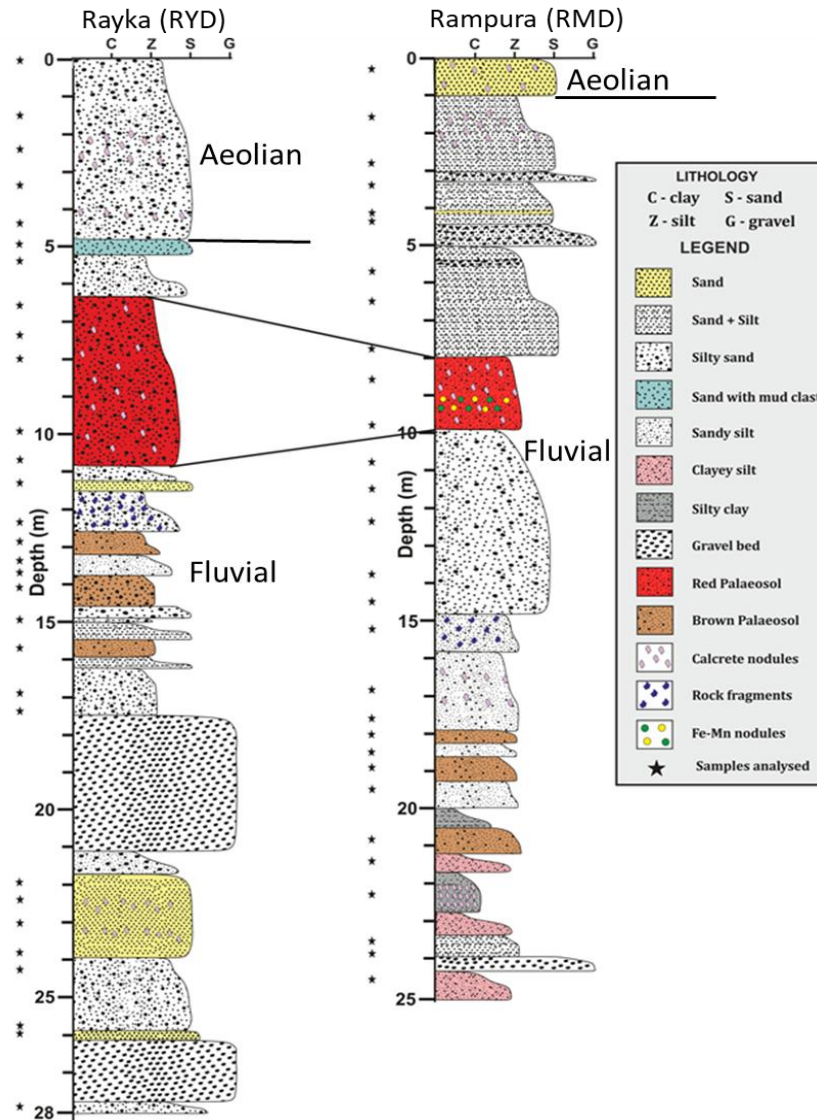


Figure 4.2: Comparative litholog of RYD and RMD cores. Depths from which samples were taken for analysis are marked with stars. Depositional environment and age are indicated as per Juyal et al. (2000).

4.2.2 Physicochemical attributes of RYD and RMD cores

Overview of physicochemical attributes of RYD and RMD cores that showed significant differences ($p < 0.01$) between both cores is represented in Fig. 4.3. Physicochemical attributes that did not show a significant difference between the two cores are not presented here. The upper region (up to 5 m) of the RMD core comprised of aeolian deposits and stratigraphic sequences of fluvial deposits had a significantly higher pH ($p < 0.01$) (ranging from 8.9 to 11.7)

as compared to the upper region of the RYD core (ranging from 8 to 9.3) that is largely comprised of aeolian deposits only. There was no significant difference observed in the pH of the lower region of both cores (ranged from 8.4 to 9.8) (Fig. 4.3). The RMD core had significantly higher bulk org. C content and significantly lower inorg. C content than the RYD core (Fig. 4.3). EC, salinity, and TDS values were significantly higher in the RMD core compared to the RYD core ($p < 0.0001$) indicates higher ionic concentration in the RMD core (Fig. 4.3). Among elemental content, significantly ($p < 0.01$) high Al_2O_3 , Fe_2O_3 , MgO, Cr, Zn, and Nd were found to be exhibited by samples of the RMD core (Fig. 4.3).

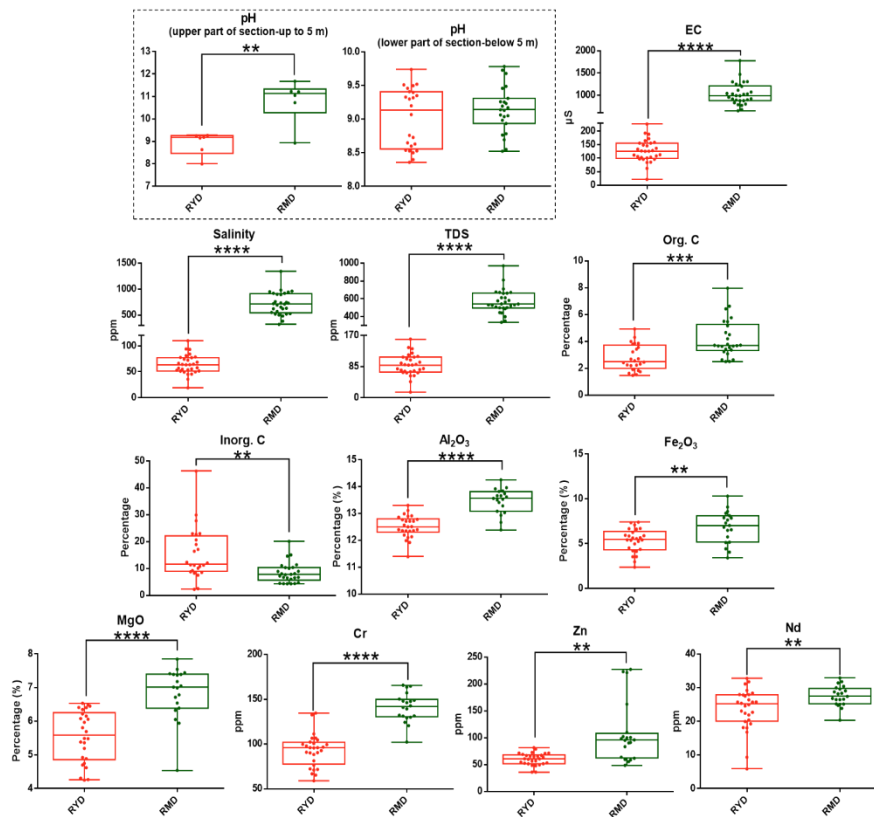


Figure 4.3: Box plots of physicochemical attributes and elemental content that showed a significant difference ($p < 0.01$) between the RYD and RMD cores. Box plots show a comparison of the median and scatter of the range of values within the entire core. The pH of the upper and the lower region of cores are represented separately in the dotted rectangle. Significant difference was determined using Welch's t-test (two-sided) (** $p < 0.01$, *** $p < 0.001$, **** $p < 0.0001$). EC: electrical conductivity, TDS: total dissolved solids, Org. C: organic carbon and Inorg. C: inorganic carbon.

4.2.3 Microbial enzyme activities and enzymatic stoichiometry within RYD and RMD cores

Dehydrogenase (DHA) activity was high ($11.5 \mu\text{g TPF g}^{-1}$ dry wt core sediment 24h^{-1}) in the top surface core sample and steeply decreased up to 3.5 m depth ($1.9 \mu\text{g TPF g}^{-1}$ dry wt core sediment 24h^{-1}) within RYD core (Fig. 4.4). Similarly, within the RMD core, DHA activity steeply decreased up to 3 m depth (9.4 to $4.7 \mu\text{g TPF g}^{-1}$ dry wt core sediment 24h^{-1}) after that no further significant reduction was observed (Tukey's test, $p > 0.05$). Protease enzyme (PTA) showed high activity in the upper horizons of the RYD core and decreased to a constant low value beyond 10 m but in the RMD samples, it was low throughout ($p < 0.0001$) (Fig. 4.4). In the RYD core, the highest β -GA activity was observed to be exhibited by the top 0.1 m depth sample ($14 \mu\text{g pNP g}^{-1}$ dry wt core sediment 2h^{-1}) while in RMD core highest β -GA activity was observed at the 6.5 m depth sample ($9 \mu\text{g pNP g}^{-1}$ dry wt core sediment 2h^{-1}) (Fig. 4.4). However, less variability in β -GA and FDA HA were observed within the RYD core while within the RMD core higher activity of these enzymes was observed in some of the deeper horizons (Fig. 4.4). Welch's t-test indicated a significant difference ($p < 0.05$) in FDA HA of both sediment core profiles (Fig. 4.4). Alkaline PA ranged from 3 to $65 \mu\text{g pNP g}^{-1}$ dry wt core sediment 2h^{-1} in RYD core samples and 10 to $62 \mu\text{g pNP g}^{-1}$ dry wt core sediment 2h^{-1} within RMD core samples. Higher Alkaline PA in many subsurface sediment samples of both sites indicates P stress in both vertical core profiles as suggested by Hill et al. (2010). There was no remarkable difference observed between RYD and RMD arylsulfatase activity ($p > 0.05$) (Fig. 4.4).

In scatter plot of coenzymatic stoichiometry, β -GA/PTA (Y axis) value observed in range of 0.2 to 3 while β -GA/Alkaline PA (X axis) value observed less than 1 in all RYD core samples, indicating P limitation throughout RYD core and C limitation in some of the RYD core samples (Fig. 4.5a). In the RMD core β -GA/PTA (Y axis) value observed greater than 1 and β -GA/Alkaline PA (X axis) value observed less than one suggesting C and P limitation in the RMD core (Fig. 4.5a). β -GA/Alkaline PA ratio observed within the range of 0.02 to 0.26 in the RYD and RMD cores indicates P limitation in both cores (Fig. 4.5b). In the RYD core, PTA/Alkaline PA ratio was observed in range of 0.018 to 0.42 and in the RMD core

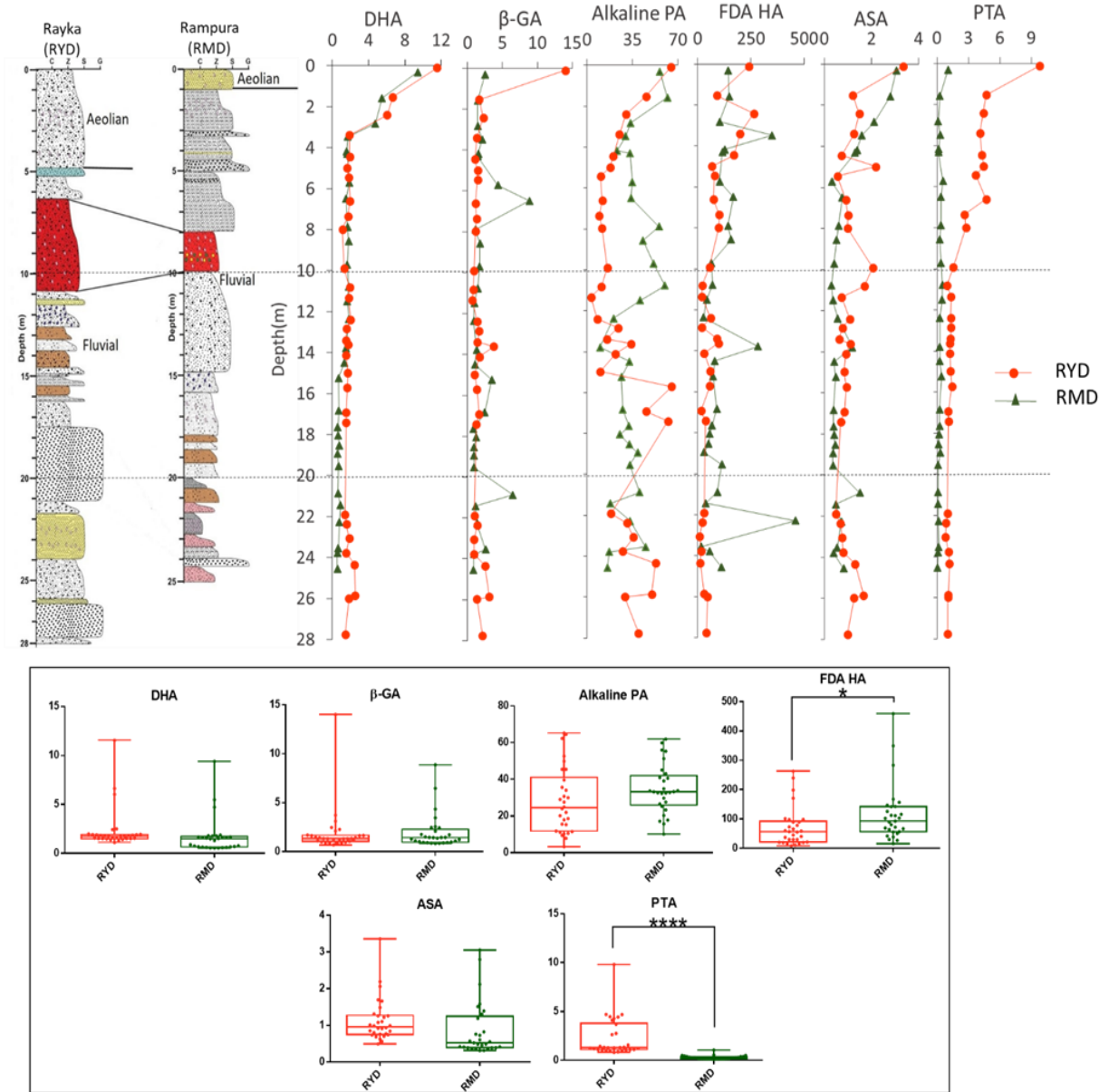


Figure 4.4: Microbial enzyme activities within RYD and RMD sediment core sections. The upper panel shows a depth-wise pattern of activities and the lower section depicts the box plots of the median and scatter values. DHA: dehydrogenase activity ($\mu\text{g TPF g}^{-1}$ dry wt core sediment 24h^{-1}), β -GA: β -D-glucosidase activity ($\mu\text{g pNP g}^{-1}$ dry wt core sediment 2h^{-1}), Alkaline PA: alkaline phosphatase activity ($\mu\text{g pNP g}^{-1}$ dry wt core sediment 2h^{-1}), FDA HA: fluorescein diacetate hydrolysis activity ($\mu\text{g fluorescein g}^{-1}$ dry wt core sediment 4h^{-1}), ASA: arylsulfatase activity ($\mu\text{g pNP g}^{-1}$ dry wt core sediment 2h^{-1}), PTA: protease activity ($\mu\text{g tyrosine g}^{-1}$ dry wt core sediment 2h^{-1}) (*p<0.05, ****p<0.0001; Welch's t-test (two-sided)).

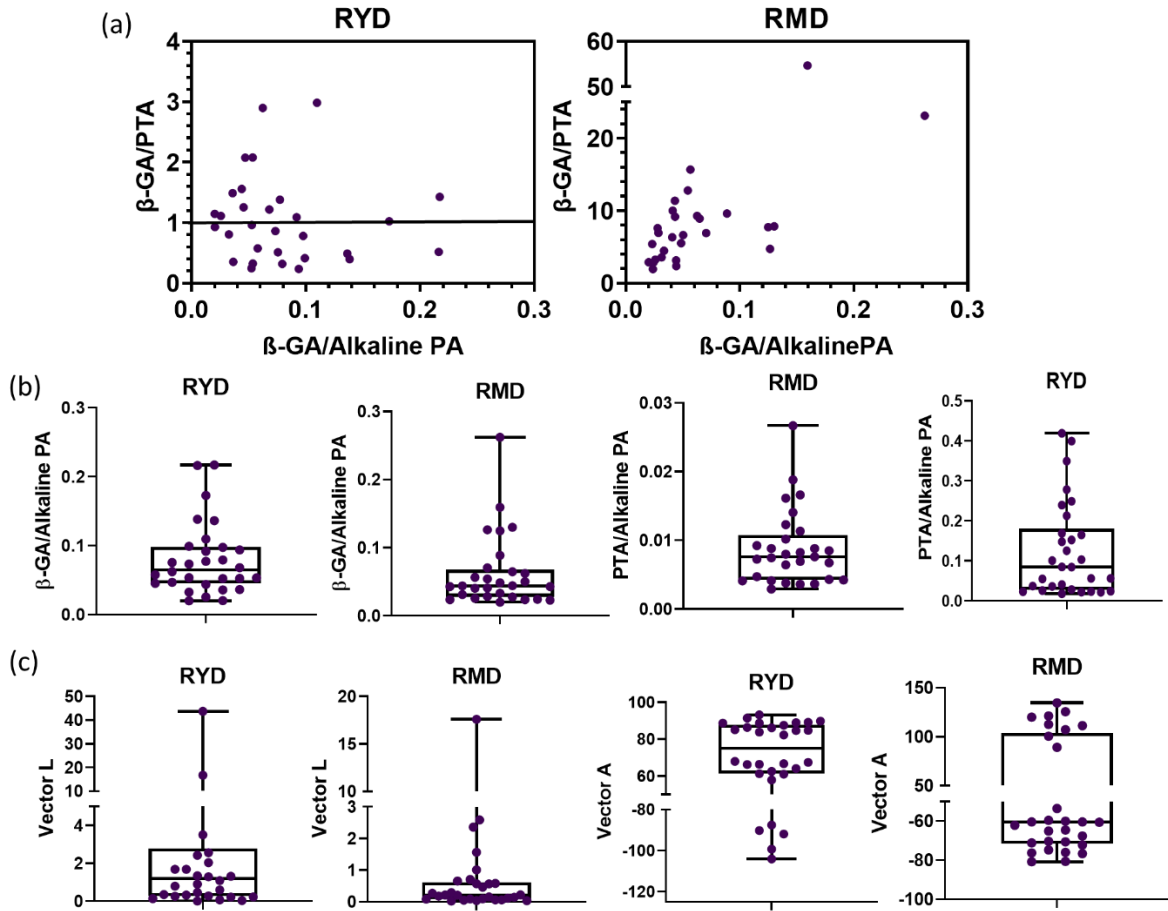


Figure 4.5: Enzymatic stoichiometry within RYD and RMD core. (a) Scatter plot of ecoenzymatic stoichiometry, with N cycle enzyme/P cycle enzyme (i.e., $\beta\text{-GA/alkaline PA}$) as the x-axis and C cycle enzyme/ N cycle enzyme (i.e., $\beta\text{-GA/PTA}$) as y-axis (b) Ratios of C cycle enzyme/ P cycle enzyme i.e. $\beta\text{-GA/Alkaline PA}$ and N cycle enzyme/ P cycle enzyme i.e. PTA/Alkaline PA (c) vector analysis of ecoenzymatic stoichiometry: vectors length (L, unitless) and vector angle (A, degree) calculated using formulas as shown below.

Vector L = $\sqrt{(\ln\beta\text{-GA}/ \ln\text{PTA})^2 + (\ln\beta\text{-GA}/ \ln\text{Alkaline PA})^2}$, Vector A = Degrees (ATAN2 (($\ln\beta\text{-GA}/ \ln\text{Alkaline PA}$), ($\ln\beta\text{-GA}/ \ln\text{PTA}$))).

PTA/Alkaline PA ratio was observed in range of 0.003 to 0.027 which also suggested P limitation in the both cores (Fig. 4.5b). Vector length (L) observed in range of 0.02 to 18 (except one sample in the RYD core that showed 43.7 value) and did not significantly differ in both cores [Welch's t-test (two-sided)]. Higher vector length values observed in some of the

RYD and RMD samples suggest C acquisition (Fig. 4.5c). Vector A differ significantly in both cores [$**p < 0.01$; Welch's t-test (two-sided)]. In the RYD core, majority of core samples showed $>45^\circ$ vector angle (except 5 samples) suggesting P limitation while in the RMD core majority of core samples (except 9 samples) showed $<45^\circ$ vector angle suggesting N acquisition in that core (Fig. 4.5c). On the whole, coenzymatic stoichiometry revealed C and P limitation in RYD core samples and C, N, and P limitation in RMD core samples.

4.2.4 Culturable bacterial counts of RYD and RMD core profiles

Plate counts on R2A agar indicated that a substantial number of heterotrophic bacteria (ranging from 1.5×10^3 to 2.7×10^5) were present in both vertical cores throughout the different depths and did not display any distinct pattern with respect to the depth of the subsurface strata of RYD and RMD. A relatively high heterotrophic count was observed in the RMD core ($p < 0.05$) (Fig. 4.6). Both RYD and RMD vertical core profiles showed abundant numbers of denitrifying bacteria; however, they were about one to two orders of magnitude lower than the heterotrophic counts in most samples (Fig. 4.6). Low counts of N_2 fixing bacteria were observed up to 4.5 m in RYD samples while they were found in relatively higher numbers up to ~11 m within the RMD core and were overall significantly ($p < 0.01$) higher in RMD (Fig. 4.6).

4.2.5 Microbial gene abundance within RYD and RMD core profiles

It is well known that a large proportion of natural microbial communities are unculturable. In order to get an idea of the total bacterial counts, one of the molecular based approaches is to quantify the abundance of the house-keeping gene 16S rRNA by qPCR. Hence gene abundance by qPCR was carried out here. Bacterial 16S rRNA gene copy numbers ranged from 1.09×10^6 to 2.43×10^7 within RYD core samples and 6.1×10^5 to 7.46×10^8 within RMD core samples. Bacterial 16S rRNA gene copy numbers were generally two to three orders of magnitude higher than the observed culturable heterotrophic bacterial count in both cores and did not display any distinct pattern with respect to the depth of the subsurface strata of RYD and RMD. Archaeal 16S rRNA gene copy numbers ranged from 7.36×10^3 to 1.28×10^5 within the RYD core and 4.85×10^4 to 6.41×10^5 within the RMD core (Fig. 4.7). A lower abundance of archaeal 16S rRNA genes was observed in both the cores in comparison to the bacterial 16S

rRNA genes. Several studies reported that denitrification is one of the major process that occur in subsurface sedimentary environments under both anaerobic and aerobic conditions (Francis et al., 1989; Rice and Rogers, 1993; Chen and Strous, 2013). Hence, copy numbers of the *nirS* gene (encoding cytochrome cd_1 -nitrite reductase - a key enzyme in denitrification) were determined. Copy numbers of *nirS* gene were observed within the range of 1×10^4 to 2.43×10^5 and 6.1×10^3 to 8.2×10^5 within RYD and RMD core respectively (Fig. 4.7). On the whole, a higher abundance of bacterial 16S rRNA, archaeal 16S rRNA, and *nirS* gene copies were found in RMD sediment samples ($p < 0.05$) (Fig. 4.7).

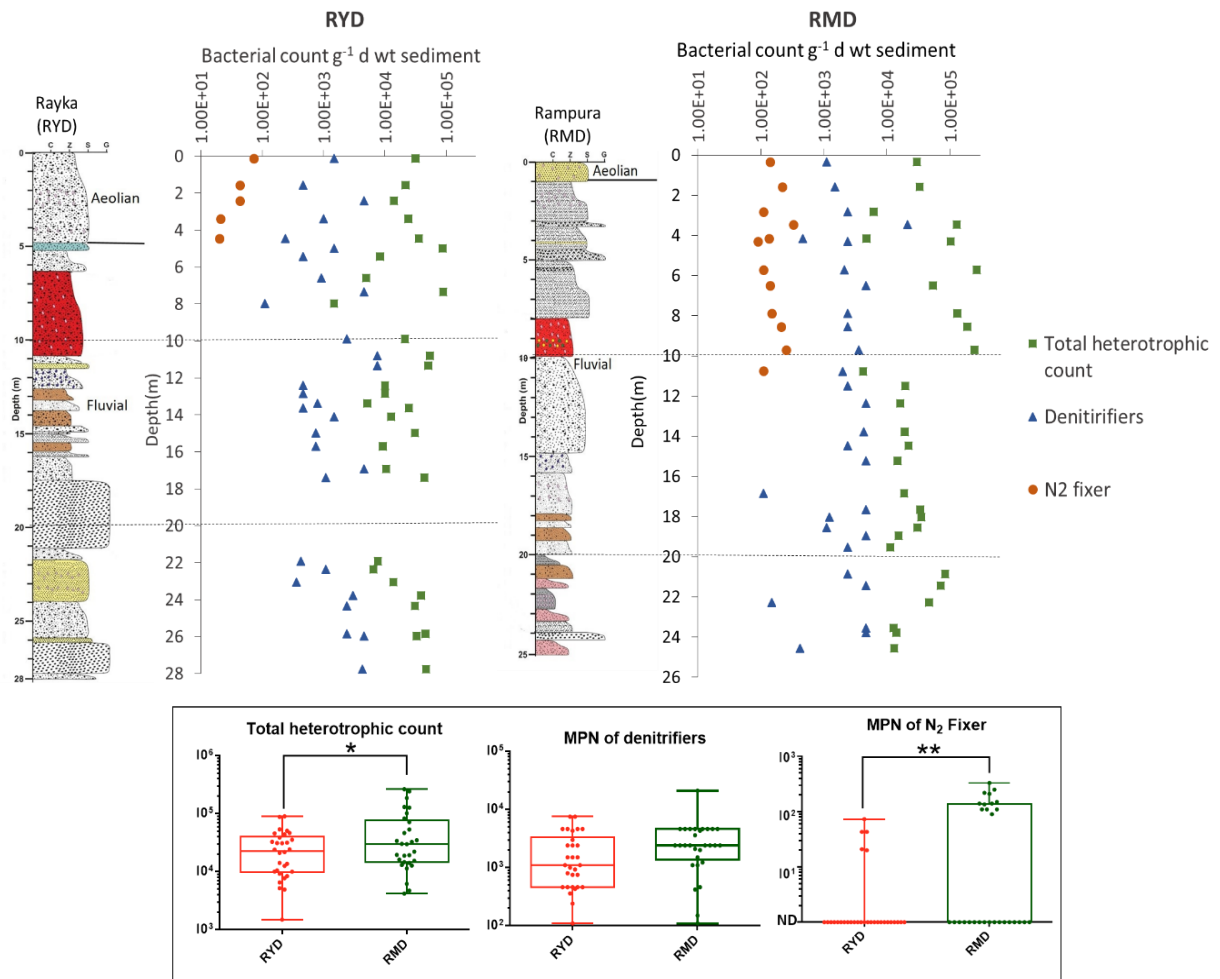


Figure 4.6: Counts of culturable bacteria in RYD and RMD cores. The upper panel shows a depth-wise pattern and the lower section depicts the box plots of the median and scatter values. Culturable bacteria were determined by plating for heterotrophic bacteria and by MPN for denitrifiers and N_2 fixers. (* $p < 0.05$, ** $p < 0.01$; Welch's t-test (two-sided)).

There was a significant difference observed in the Zn content of both core profiles (Fig. 4.3). Therefore, *czcA* gene abundance was also determined. As earlier reported the CzcA gene encodes for an inner membrane antiporter cation carrier of a Co/Zn/Cd efflux pump and that confers resistance against heavy metals Co^{2+} , Zn^{2+} , and Cd^{2+} (Roosa et al. 2014). The abundance of the *czcA* gene was observed within the range of $<10^3$ to 10^4 in both sediment cores, however, most samples showed no detectable ($<10^3$) *czcA* gene copies in the RYD core as compared to the RMD core (Fig. 4.7).

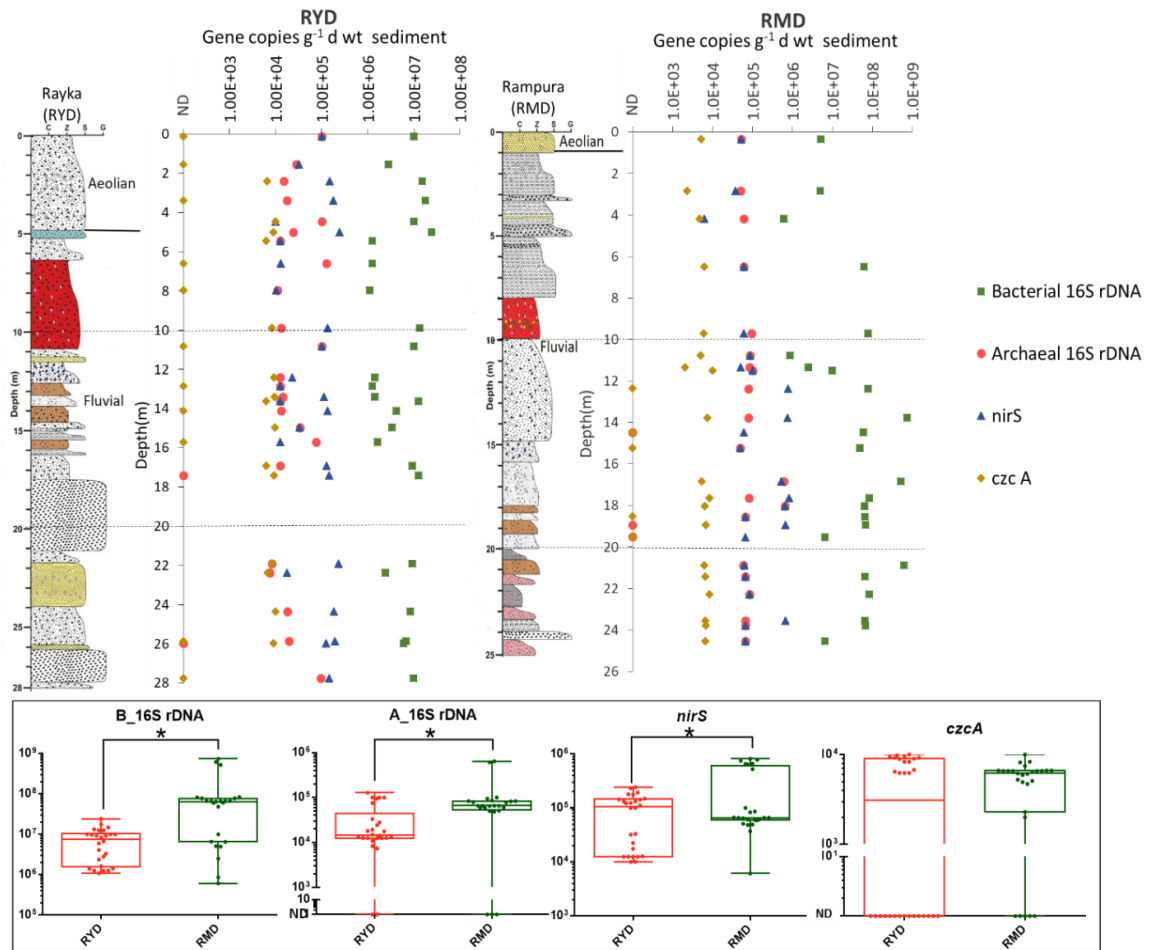


Figure 4.7: Gene abundances within RYD and RMD core samples by qPCR. The upper panel shows a depth-wise pattern and the lower section depicts the box plots of the median and scatter values. Samples in which gene abundance was below the detection limit ($<10^3$) represented as ND (not detected). (* $p < 0.05$; Welch's t-test (two-sided)). B_16S rDNA: bacterial 16S rRNA gene abundance, A_16S rDNA: archaeal 16S rRNA gene abundance.

4.2.6 Linkage between and within microbial and geological characteristics of RYD and RMD cores

To determine the linkage between and within microbial, elemental, and physicochemical characteristics principal component analysis (PCA) was performed (Fig. 4.8, 4.9). To understand which geological variables strongly influence microbiological characteristics in the two cores, Pearson's correlation analysis was done (Fig. 4.10). As expected, moisture content exhibited a positive correlation with clay content and negative correlation with sand content;

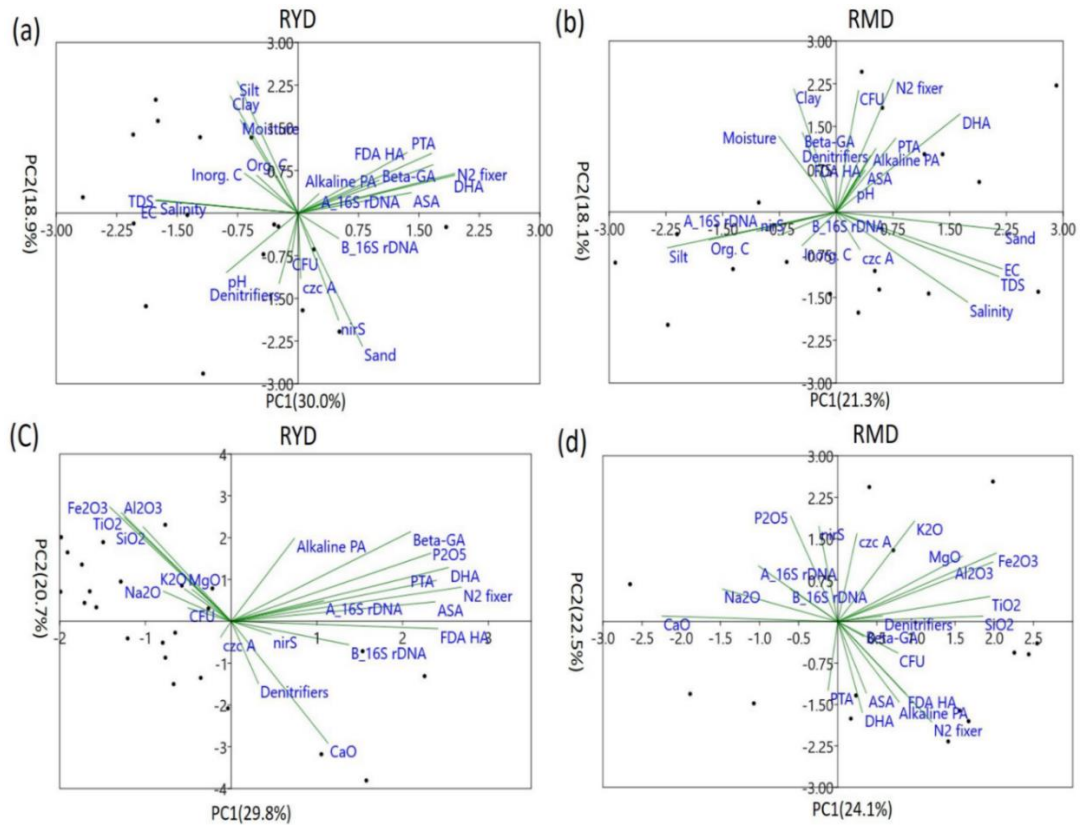


Figure 4.8: Principal component analysis (PCA) of physicochemical attributes, grain size distribution data and major oxides with microbial characteristics within RYD and RMD core profiles. PCA between physicochemical attributes, grain size distribution data, and microbial characteristics within (a) RYD and (b) RMD. PCA between major oxides and microbial characteristics within (c) RYD and (d) RMD. A_16S rDNA: archaeal 16S rRNA gene abundance, B_16S rDNA: bacterial 16S rRNA gene abundance, Beta-GA: β -D-glucosidase activity, CFU: total heterotrophic count. The remaining other abbreviations are the same as mentioned in the text.

EC, TDS, and salinity clustered close together in both cores (Fig. 4.8a, 4.8b). All major oxides clustered together except P₂O₅, CaO (which clustered distinctly in both cores), and Na₂O (which clustered distinctly in RMD core only) (Fig. 4.8c, 4.8d). All trace elements clustered together and exhibited positive correlations with each other except Sr and Nb in the RYD core. While, in the RMD core, V, Th, Nb, Ni, Hf, and Rb exhibited a positive correlation with each other and Sr, Zn, U, as well as Cr clustered distinctly (Fig. 4.9a, 4.9b). Likewise, within the RYD core, all REEs clustered together while within the RMD core Er and Ce clustered distinctly with respect to remaining other REEs (Fig. 4.9c, 4.9d). Among microbial characteristics, all enzyme activities and N₂ fixer count clustered together while gene abundance, total heterotrophic counts, and denitrifying bacterial counts clustered distinctly (Fig. 4.8, 4.9).

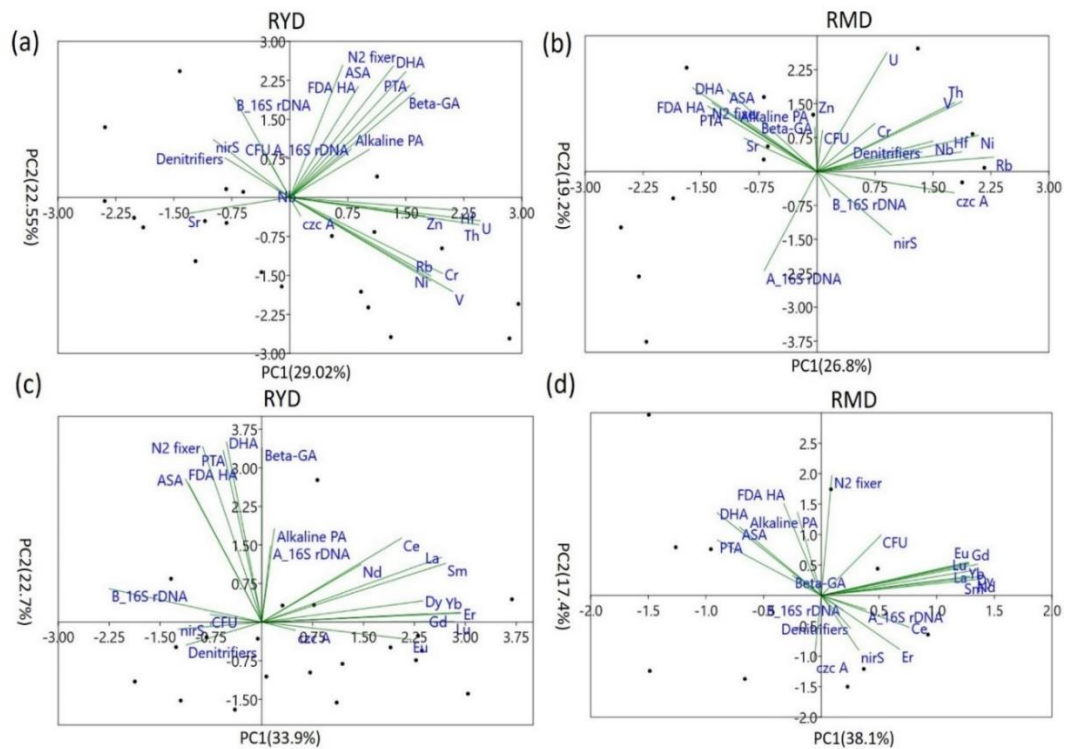


Figure 4.9: Principal component analysis (PCA) of trace elements and rare earth elements (REEs) with microbial characteristics within RYD and RMD core profiles. PCA between trace elements and microbial characteristics of the (a) RYD and (b) RMD. PCA between REEs and microbial characteristics of the (c) RYD and (d) RMD. Abbreviations are the same as mentioned in Fig. 4.8.

Figure 4.10 at a glance shows that geochemical parameters that are well correlated (positively or negatively) with microbial activities differ in both the cores. For instance, EC, TDS, and salinity exhibit a negative influence on DHA, β -GA, alkaline PA, and N_2 fixer count; P_2O_5 content shows a positive correlation with all microbial enzyme activities except phosphatase activity in the RYD core. *NirS* gene abundance is high in sandy samples while low in silty or clayey samples in RYD core (Fig. 4.10). In addition, several other parameters showed a moderate correlation in RYD samples. All trace elements and REEs clustered distinctly with respect to microbial enzyme activities and did not exhibit correlation with microbial enzyme activities (except Sr which exhibits a negative correlation with PTA) within the RYD core (Fig. 4.9a, 4.9c, 4.10). Conversely, bacterial 16S rRNA gene abundance exhibited a negative association with trace elements and REEs within the RYD core (Fig. 4.9a, 4.9c) while archaeal 16S rRNA gene abundance did not show a significant correlation with any investigated geological variables within the RYD core (Fig. 4.10).

In the RMD core, although EC, TDS, and salinity levels were significantly higher than the RYD core (Fig. 4.3), these parameters did not exhibit a significant correlation with enzyme activities (except PTA which exhibit a weak positive correlation with EC). Inorganic C content exhibited a strong positive correlation with archaeal 16S rRNA gene abundance and a weak negative correlation with denitrifying bacterial counts in RMD core while in RYD core inorg. C content did not exhibit a significant correlation with any microbial characteristics studied in this work. P_2O_5 exhibited a strong negative correlation with N_2 fixer count and a weak negative correlation with phosphatase activity (which is contradictory to the relationship observed at RYD core) as well as with total heterotrophic count. K_2O exhibits a weak positive correlation with *nirS* gene abundance in RMD while it was moderate negative in the case of RYD.

Bacterial 16S rRNA gene abundance had no significant correlation with any investigated geological variables within the RMD core, which is also contradictory to that observed at the RYD core (Fig. 4.10). Several REEs exhibited a weak negative correlation with DHA and PTA activity in the RMD core (Fig. 4.10, 4.9d). A significant negative correlation of Ni with bacterial 16S rRNA gene abundance, *nirS* gene abundance, and the denitrifying bacterial count was observed in the RYD core. On the other hand in the RMD core, Ni content did not show significant relation with the above microbial parameters (Fig. 4.10). Additionally, *czcA* gene

abundance showed a significant positive correlation with Ni content in the RMD core profile but not in the RYD core profile.

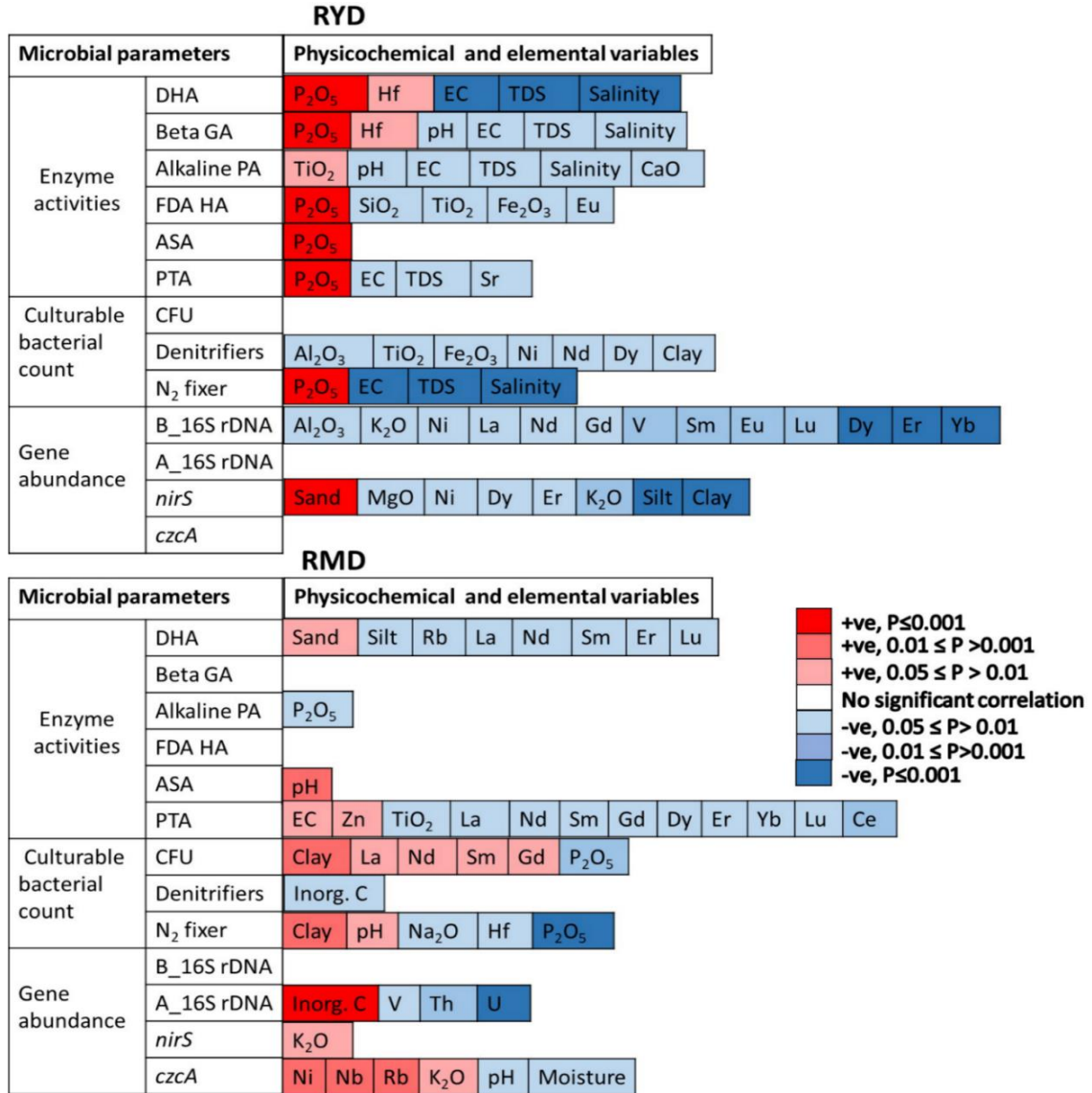


Figure 4.10: Pearson’s correlations of microbial parameters with geological variables within RYD and RMD vertical core sections. Color coding indicates a positive or negative correlation with their level of significance as shown in the right-hand side legend. Beta GA: β-D-glucosidase activity, CFU: total heterotrophic count, B_16S rDNA: bacterial 16S rRNA gene abundance, A_16S rDNA: archaeal 16S rRNA gene abundance. The remaining other abbreviations are the same as mentioned in the text.

4.3 Discussion

In the present study, we determined microbial enzyme activities, gene abundance, culturable counts, and their correlation with sediment indigenous properties such as grain size distribution, the content of 29 different elements; bulk org. C, bulk inorg. C and moisture content; pH, EC, salinity, and TDS. Among enzyme activities determined here, the only dehydrogenase is an intracellular enzyme associated with actively growing/respiring microbial population or living biomass (Mosher et al. 2003; Marcos et al. 2020) remaining other enzymes are extracellular and independent to the magnitude of actually actively respiring or metabolizing microbial population because they can also be associated with cell debris or dead cells, absorbed or sequestered by soil particles and remain stable (Dilly and Nannipier 1998). However, extracellular enzymes provide a vital understanding of microbial roles in various biogeochemical cycling processes (Das and Varma 2011). Dehydrogenase activity decreases steeply in both cores indicating a reduction in actively growing/respiring microbial population with depth but several deeper samples of both cores exhibit high alkaline PA and FDA HA activities (Fig. 4.4) indicated the substantial role of both core ecosystems in biogeochemical cycling. Ecoenzymatic stoichiometry revealed nutrient acquisition in both cores might be due to older sediment deposition and lower nutrient transportation the subsurface owing to low groundwater recharge rate in semiarid climate.

Culturable bacterial counts and bacterial 16S rRNA gene abundance were found in significant numbers throughout the depth of both the core samples and did not display any distinct pattern with respect to the depth of the subsurface strata of RYD and RMD. This is in accordance with other reports for glacio-fluvial sediments of the Quaternary period located near the Vejen city, Denmark (Albrechtsen and Winding 1992), three boreholes drilled at the U. S. Department of Energy's Savannah River Plant (SRP) in South Carolina (Fredrickson et al. 1989) and Quaternary sediments cores of the tidal-flat area of Spiekeroog Island, Germany (Beck et al. 2011) where greater microbial abundance was reported even at deep subsurface. Contradictory to that, a decrease in microbial biomass with increasing depth has been reported by Fierer et al. (2003) for the valley and terrace soil profiles comprising weakly consolidated Quaternary alluvium of Santa Ynez River (California, USA). In present work, lower abundance of archaeal 16S rRNA genes than bacterial 16S rRNA genes within both RYD and RMD cores (Fig. 4.7)

indicate dominance of bacterial population in subsurface cores of the Mahi river basin. Lin et al. (2012) and Beck et al. (2011) also demonstrated a lower abundance of archaeal 16S rRNA genes than bacterial 16S rRNA genes within 52 m deep vertical stratigraphic core of Hanford site, Washington (USA) and 20 m deep coastal Quaternary sediments cores of Spiekeroog Island, Germany respectively.

Denitrification process [reduction of nitrate (NO_3^-) or nitrite (NO_2^-) into the various N gases] of natural terrestrial biosphere accounts for the loss of ~ 28 Tg of N/yr via N_2 efflux (Houlton and Bai 2009) and is regulated by physicochemical characteristics such as availability of oxygen, nitrate, carbon, pH, salinity content of soil/sediment (Groffman 2012). A higher abundance of denitrifying populations within subsurface ecosystems is reported by Yeomans et al. (1992) in Iowa subsoils (up to 3 m depth) and Hashimoto et al. (2006) in the subsurface upland soil by MPN method. Jiang et al. (2017) reported 0.37 to 44.08×10^8 *nirS* gene copies g^{-1} sediment via qPCR in surface sediment samples of 22 lakes situated at the middle and lower Yangtze River basin. In this study, we report the presence of viable denitrifying bacteria as well as their gene (*nirS*) up to a depth of 28 m and their contrasting correlation with geological variables in both cores of the Mahi River (Fig. 4.6, 4.7, 4.10). The denitrifying bacterial guilds might be distinct in both cores considering that more than 60 genera are known to carry out denitrification (Philippot et al. 2007), this could be a reasonable possibility for contrasting correlation.

In this study, we also determined the abundance of *czcA* gene ranged from 0 (not detected) to 659 copies per 10^5 16S rRNA gene copies within RYD core samples [total Zn content ranging from 35.9 to 81.4 ppm] and 0 (not detected) to 774 copies per 10^5 16S rRNA gene copies within RMD core samples [total Zn content ranging from 48.4 to 227 ppm]. Chen et al. (2019) demonstrated *czcA* gene copies range from $4.51(\pm 1.59)$ to $19.74 (\pm 10)$ per 10^5 16S rRNA gene copies in soil samples with a total Zn content range from 14.5 to 113 ppm. Additionally, in both RYD and RMD core profiles, *czcA* gene abundance did not exhibit significant correlation with a total Zn content (Fig. 4.10). All this suggests that high total Zn content does not necessarily imply the presence of high *czcA* gene copies but a complex interplay of factors such as metal speciation and bioavailability of metal have an influence on

metal tolerance ability of bacteria which might ultimately correlate with metal resistant gene abundance (Giller et al. 2009; Roosa et al. 2014).

As mentioned above, gene abundance and culturable counts (except N₂ fixer) did not clearly display a depth dependent pattern in both cores, while microbial enzyme activities exhibited a distinct depth associated pattern (Fig. 4.4, 4.6, 4.7). Moreover, microbial enzyme activities clustered distinctly in PCA analysis with respect to microbial abundance [i.e. gene abundance and culturable counts (except N₂ fixer)] (Fig. 4.8, 4.9) which indicates that high bacterial abundance did not necessarily denote high enzyme activities in subsurface sediment samples but they might be regulated or influenced by sediment physicochemical and geological characteristics or differences in microbial community composition (Turner et al. 2014; Schnecker et al. 2015).

Among physicochemical characteristics, bulk org. C content did not show a significant correlation with any microbial parameters studied here and a negative correlation of salinity with several microbial enzyme activities was observed in the RYD core while within the RMD core no significant correlation of salinity with microbial enzyme activities was observed (Fig. 4.10) even though significantly higher salinity was observed in this core profile. This finding indicated that bulk total org. C is not the key determinant in influencing microbial characteristics within both cores of the Mahi River basin. This might be because of not only quantity but the quality of org. C is also imperative for the subsurface microbial characteristics (Fischer et al. 2002; Freixa et al. 2016). Additionally, we did not observe a depth dependent gradient in bulk total org. C content of both cores (data not shown) because bulk total org. C content generally depends on depositional sources and sedimentary depositional conditions (Blair et al. 2004; Koiter et al. 2015). Although various earlier studies have investigated the influence of salinity on microbial enzyme activities, their results are not always consistent. For instance, Pan et al. (2013) and Siddikee et al. (2011) reported detrimental effects of salinity on various extracellular enzyme activities of grassland and coastal soils respectively. On the other hand, Frankenberger and Bingham (1982), Saviozzi et al. (2011), Morrissey et al. (2014) demonstrated salinity enhanced, suppressed, or unaffected various microbial enzyme activities. However, the influence of salinity is dependent on site specific availability of specific ions and salts, osmotic potential of the soil-water phase as well as on the type of enzyme (Pan et al. 2013;

Frankenberger and Bingham 1982). Here we also observed a divergent relationship of salinity in both cores which may reflect specific adaptation of the microbial community towards high salinity in the RMD core.

Several major oxides also exhibited different correlations with the same microbial parameters in both core samples e.g. correlation of P_2O_5 with microbial enzyme activities, K_2O with *nirS* gene abundance (Fig. 4.10). It is of interest to note that K_2O content did not vary significantly in both cores yet this oxide exhibited a contradictory correlation with *nirS* gene abundance in both cores. Numerous other major oxides exhibit a negative correlation with microbial parameters in both cores with the exception of the positive correlation observed between TiO_2 and alkaline PA in the RYD core. A strong positive correlation of P_2O_5 with microbial enzyme activities observed in the RYD core is in agreement with previous findings on exposed Rayka sediments (Subrahmanyam et al. 2021). This study also reported a negative impact of SiO_2 , positive impact of Fe and Al oxides of microbial activity in exposed alluvial sediments of the Mahi river Basin (Subrahmanyam et al. 2021). Contradictory to that, Turner et al. (2014) reported an adverse effect of poorly crystalline Fe and Al oxides on microbial enzyme activities in mineral soil horizons situated along the 120 kyr old Franz Josef chronosequence (New Zealand). In the present study, we also observed the negative impact of Fe and Al oxides.

A negative impact of trace elements such as Ni, Cr, Cu, Pb, Zn on microbial enzyme activities has been reported in the Ganga riverbed sediment (India) (Jaiswal and Pandey 2018; Verma and Pandey 2019). Nema et al. (2019) revealed positive and negative associations of various trace elements including Hf and Sr with the abundance of different bacterial phyla in deep subsurface sediments of the Krishna Godavari basin (India). Here we observed a significant positive correlation of trace element Hf with dehydrogenase, β -glucosidase activity, and a moderate negative correlation of Sr with protease activity in the RYD core. Together with this, a negative correlation of Ni with bacterial 16S rRNA gene abundance, *nirS* gene abundance, and the denitrifying bacterial count was also observed in the RYD core. On the other hand in the RMD core, Ni content did not show significant relation with the above microbial parameters (Fig. 4.10) Moreover, *czcA* gene abundance did not exhibit a significant correlation with total Zn content in both cores but showed a significant positive correlation with Ni in the RMD core (Fig. 4.10). Roosa et al. (2014) also reported a positive correlation of non-

targeted metals including Ni with *czcA* gene abundance. How non-targeted metals influence *czcA* gene abundance is not understood. Although several trace elements have been studied for their influence on microbial parameters, *in situ* interaction of a wide array of other trace elements with microbial characteristics in stratified river floodplain ecosystems is not reported. In the present work, we reported a positive correlation of Rb and Nb with *czcA* gene abundance while a negative correlation of V, Th, U with archaeal 16S rRNA gene abundance and also a negative correlation of Rb with DHA in the RMD core.

Rare earth elements such as La, Nd, Dy, Gd, Sm, Er, Yb, Eu, Lu showed a negative correlation with several microbial parameters in both cores except total heterotrophic count (CFU) (positively correlated with REEs) in the RMD core (Fig. 4.10). Chu et al. (2003) reported adverse effects of La on microbial dehydrogenase activity of red soil samples collected from crop land of the Chinese Academy of Sciences. Phosphate solubilising microbes solubilized rare earth phosphate mineral monazite and released REEs to the surrounding area (Corbett et al. 2017). The impact of REEs including La, Ce, Er on the microbial community composition at Krishna Godavari basin (India) has been demonstrated by Nema et al. (2019). Although a positive and negative impact of specific elements on microbial parameters is reported for different environments, the mechanism or reason behind such correlation is unknown. In this study, we observed distinctive correlation patterns in the RMD and RYD core samples and also in exposed alluvial sediments (Subrahmanyam et al. 2021). Such phenomena observed might be due to different dynamics of *in situ* mineral-microbes interactions and/or discrepancy in bioavailability of elements in both the cores and exposed sediments.

4.4 Conclusion

The geological complexities of subsurface stratified sediment sequences of the Mahi River basin were used as a model to understand the inter-relationship between microbial parameters with geological characteristics. The microbial enzyme activities revealed that both river terraces sedimentary profiles play a significant role in C, N, P, and S biogeochemical cycles. Ecoenzymatic stoichiometry revealed C and P limitation in RYD core samples and C, N, and P limitation in RMD core samples. Principal component analysis and Pearson's correlation analysis indicate significant linking of specific geochemical factors with microbial parameters

in both the core profiles. However, the strength and direction (positive or negative) of correlation varied between the two sediment profiles. Notable among these were the strong positive relationship between P_2O_5 content and various enzyme activities and negative correlation of salinity and pH with enzyme activities in RYD core but not in RMD core. Likewise, a positive correlation between Ni and *czcA* gene abundance was observed in the RMD core but not in the RYD core. These results emphasize that sediment geochemical properties correlate differently with microbial parameters in the Late Quaternary subsurface sediment sequences. It would be interesting to study further the potential reasons for this distinguishable correlation pattern observed in both cores. Additionally, this work could assist future investigation on the alternation of microbial activity via deviating abiotic factors that link with microbial parameters to improve sediment ecosystem functioning of the region.